JBC RESEARCH ARTICLE

Exostosin glycosyltransferase 1 reduces porcine reproductive and respiratory syndrome virus infection through proteasomal degradation of nsp3 and nsp5

Received for publication, December 15, 2021 Published, Papers in Press, December 28, 2021,
https://doi.org/10.1016/j.jbc.2021.101548

Xiaoxiao Zhang[‡], Wenjuan Dong[‡], Xun Wang, Zhenbang Zhu, Sheng He, Hui Zhang, Yaosheng Chen, Xiaohong Liu, and Chunhe Guo[*]

From the State Key Laboratory of Biocontrol, School of Life Sciences, Sun Yat-sen University, Guangzhou, Guangdong, PR China

Edited by Craig Cameron

Porcine reproductive and respiratory syndrome virus (PRRSV) continues to be a serious threat to the swine industry worldwide. Exostosin glycosyltransferase 1 (EXT1), an enzyme involved in the biosynthesis of heparin sulfate, has also been reported to be a host factor essential for a wide variety of pathogens. However, the role of EXT1 in PRRSV infection remains uncharted. Here, we identified that PRRSV infection caused an increase of EXT1 expression. EXT1 knockdown promoted virus infection, whereas its overexpression inhibited virus infection, suggesting an inhibitory function of EXT1 to PRRSV infection. We found that EXT1 had no effects on the attachment, internalization, or release of PRRSV but did restrict viral RNA replication. EXT1 was determined to interact with viral nonstructural protein 3 (nsp3) and nsp5 *via* its N-terminal cytoplasmic tail and to enhance K48-linked polyubiquitination of these two nsps to promote their degradation. Furthermore, the C-terminal glycosyltransferase activity domain of EXT1 was necessary for nsp3 and nsp5 degradation. We also found that EXT2, a EXT1 homolog, interacted with EXT1 and inhibited PRRSV infection. Similarly, EXT1 effectively restricted porcine epidemic diarrhea virus and porcine enteric alphacoronavirus infection in Vero cells. Taken together, this study reveals that EXT1 may serve as a broad-spectrum host restriction factor and suggests a molecular basis for the potential development of therapeutics against PRRSV infection.

Porcine reproductive and respiratory syndrome (PRRS) is an economically significant infectious disease of swine herds characterized by severe reproductive failure in sows and respiratory distress in piglets and growing pigs (1, 2). PRRS virus (PRRSV), the etiologic agent, is a small and enveloped positive-stranded RNA virus classified within the order Nidovirales, family Arteriviridae, and genus *Arterivirus* (3, 4). Two distinct species of PRRSV, designated "European" (PRRSV-1) and "North American" (PRRSV-2), have been well described, which share approximately 60% sequence identity (1, 5). Pigs attacked by either PRRSV-1 or PRRSV-2 present with inappetence, fever, lethargy, and respiratory distress (6). Since the initial outbreaks of PRRS in the late 1980s, tremendous efforts have been made to control this disease. However, PRRSV prevention has still been in a dilemma because of the constantly evolving and immunosuppressive properties of this virus (7).

Exostosin glycosyltransferase 1 (EXT1) is a member of EXT family of glycosyltransferases, which takes part in the biosynthesis of heparin sulfate (HS) (8). So far, five genes encoding EXT proteins have been identified in mammals, EXT1, EXT2, EXTL1, EXTL2, and EXTL3. EXTs share a similar structure and are all single-pass membrane proteins. Except for EXTL1, these proteins ubiquitously expressed in mammalian tissues (8). Mutations in either EXT1 or EXT2 result in hereditary multiple osteochondromas (9). The recent study has described an important role of EXT1 in the early stage of Filovirus entry (10). And genome-wide CRISPR screening identified that EXT1 is required for severe acute respiratory syndrome respiratory syndrome coronavirus 2, dengue virus, Zika virus, and Japanese encephalitis virus infection (11–13). Similarly, the HS synthesis function of EXT1 has been validated to contribute to vaccinia virus infection (14). It is not clear whether EXT enzymes own other biological functions in addition to HS polymerization. What is more, the role of EXT enzymes in PRRSV infection has not been reported yet.

Here, we aimed to examine the role of EXT1 in PRRSV infection. We discovered that EXT1 was constitutively expressed and further upregulated upon PRRSV infection in both Marc-145 cells and porcine alveolar macrophages (PAMs). EXT1 silence enhanced PRRSV infection, whereas overexpression suppressed PRRSV infection, suggesting that EXT1 functions as a restriction factor to PRRSV. EXT1 had no effects on PRRSV attachment, internalization, or release but took part in viral RNA replication. Three residues, Asn-651, Asp-654, and Arg-701, within the C-terminal glycosyltransferase activity domain of EXT1 were indispensable for its antiviral function. EXT1 interacted with viral nonstructural protein 3 (nsp3) and nsp5 *via* its N-terminal cytoplasmic tail and reduced these two nsps through promoting their K48-linked polyubiquitination. Impaired nsp3 and nsp5 might restrain the formation of viral replication transcription complex (RTC), thus inhibiting the RNA replication of PRRSV.

[‡] These authors contributed equally to this work.
[*] For correspondence: Chunhe Guo, guochunh@mail.sysu.edu.cn.

Furthermore, we found that the C-terminal glycosyltransferase activity domain of EXT1 was responsible for its nsp3 and nsp5 degradation. We also found that EXT1 inhibited porcine epidemic diarrhea virus (PEDV) and porcine enteric alphacoronavirus (PEAV) infection in Vero cells, suggesting for a probable broad-spectrum antiviral function of EXT1.

Results

PRRSV infection causes an increase of EXT1 expression in vitro

We first assessed whether PRRSV infection affects EXT1 expression. Upon PRRSV-CH-1a infection, the mRNA and protein levels of EXT1 in Marc-145 cells elevated by 3- to 15-fold and 1.4- to 2.2-fold, respectively, when compared with uninfected mock-treated cells at various hours postinfection (hpi) (Fig. 1, *A* and *B*). And at various multiplicities of infection (MOIs), the mRNA and protein of EXT1 enhanced 2- to 3-fold and 1.7- to 2-fold (Fig. 1, *C* and *D*). Furthermore, we found similar increases of EXT1 transcript levels in Marc-145 cells infected with PRRSV-enhanced GFP (EGFP) and PRRSV-TJM strains (Fig. 1*A*). The immunofluorescence analysis also demonstrated an obvious increase of EXT1 expression in PRRSV-CH-1a–infected Marc-145 cells (Fig. 1*E*). Consistent with the phenotypes observed in Marc-145 cells, PRRSV-CH-1a infection elevated EXT1 expression at mRNA and protein levels in PAMs at various hpi by 2.5- to 4-fold and 1.3- to 1.8-fold, respectively (Fig. 1, *F* and *G*). Taken together, these results indicate that PRRSV infection upregulates the expression of EXT1 in both Marc-145 cells and PAMs, arguing for a role of EXT1 during PRRSV infection.

EXT1 knockdown enhances PRRSV infection

To gain insights into the role of endogenous EXT1 on PRRSV infection, we measured viral proliferation upon EXT1 knockdown using siRNAs in Marc-145 and PAM cells. All the three independent siRNAs significantly impaired the transcript level of EXT1 at 24 h post-transfection. siRNA2 targeting EXT1 with the highest knockdown efficiency was selected for subsequent experiments (Fig. 2, *A* and *B*). Marc-145 cells or PAM cells were transiently transfected with siRNA2 or si-Ctrl for 24 h and then infected with PRRSV at an MOI of 0.5 for various times. As shown in Figure 2, *D*, *E*, *G*, and *H*, EXT1 depletion efficiently elevated the expression of viral N at both mRNA and protein levels in Marc-145 cells (Fig. 2, *D* and *E*) and PAM cells (Fig. 2, *G* and *H*) during the course of infection. Furthermore, the absolute RT–quantitative PCR (qPCR) analysis demonstrated that EXT1 knockdown increased the viral copy numbers in Marc-145 cells (Fig. 2*C*), and a higher virus titer was observed in Marc-145 cells and PAM supernatants with EXT1 knockdown (Fig. 2, *F* and *I*). These results suggest that endogenous EXT1 may restrict PRRSV infection *in vitro*.

Overexpression of EXT1 inhibits PRRSV infection

To further corroborate the role of host restriction factor of EXT1 in PRRSV infection, Marc-145 cells were transiently transfected with a Myc-tagged EXT1 plasmid or an empty vector for 36 h prior to infection with PRRSV at an MOI of 0.5 for various times. Western blot analysis revealed a robust increase in the amount of EXT1 in EXT1-overexpressing cells (Fig. 3*A*). Upon infection, the viral copy numbers and the mRNA and protein levels of viral N were obviously inhibited at various time points by the overexpression of EXT1 (Fig. 3, *B–D*). The reduced virus in Marc-145 cells with EXT1 overexpression was further demonstrated by the immunofluorescence assay (Fig. 3*E*). EXT1 overexpression also drastically decreased the virus titers in Marc-145 cell supernatants (Fig. 3*F*).

The C-terminal glycosyltransferase activity domain harbors residues responsible for the antiviral function of EXT1

As a type II membrane protein, EXT1 mainly resides in Golgi and endoplasmic reticulum (ER) apparatus membrane and is composed of an N-terminal cytoplasmic tail, a transmembrane (TM) domain, a stalk (Ext), and a large globular domain (GT64) that is likely to harbor glycosyltransferase activity in C-terminal region (15) (Fig. 4*A*). We were interested in whether the glycosyltransferase activity of EXT1 is involved in its PRRSV inhibition. To demonstrate this hypothesis, truncation mutant plasmids (EXT1-D1 and EXT1-D2) with the C-terminal domain deletion were prepared and transfected into Marc-145 cells. EXT1-D1 and EXT1-D2 were shown to express well in Marc-145 cells as assessed by Western blot (Fig. 4*C*). Transfected cells were then challenged with PRRSV at an MOI of 0.5 for 36 h. Compared with EXT1-WT, C-terminal domain deletion completely abrogated the inhibition of EXT1 on viral infection (Fig. 4, *B* and *C*). Similarly, the C-terminal domain–deleted EXT1-D1 and EXT1-D2 no longer had effect on the infectious PRRSV yield in supernatants (Fig. 4*D*). These results suggest that the C-terminal glycosyltransferase activity domain of EXT1 is vital for the suppression of PRRSV infection.

Although the exact mechanism by which EXT proteins transfer glycosyl to the HS polymer remains confusing (8, 16), aspartic acid–any amino acid–aspartic acid (DXD) motif shared by many glycosyltransferases has been demonstrated important for this process (17). Here, an inspection of the primary sequences of monkey EXT1 protein expectedly revealed an aspartic acid–glutamic acid–aspartic acid (DED) motif within the C-terminal active domain (Fig. 4*E*). To probe into the role of the DED motif in PRRSV infection, we introduced single and double aspartic-to-alanine substitutions into the WT EXT1 plasmid (D565A and D565A–D567A) as displayed in Figure 4*F* and found that neither the single nor double mutant impaired EXT1 expression (Fig. 4*H*). Similar to EXT1-WT, both mutants resulted in inhibition effects on PRRSV as measured by mRNA and protein levels of PRRSV N (Fig. 4, *G* and *H*). These results suggest that the DED motif within the C-terminal active domain of monkey EXT1 does not affect PRRSV infection.

Sequence alignment revealed that EXT proteins are highly conserved, especially in their C-terminal catalytic domain (Fig. 4*E*). Encouraged by the X-ray crystal structure of the

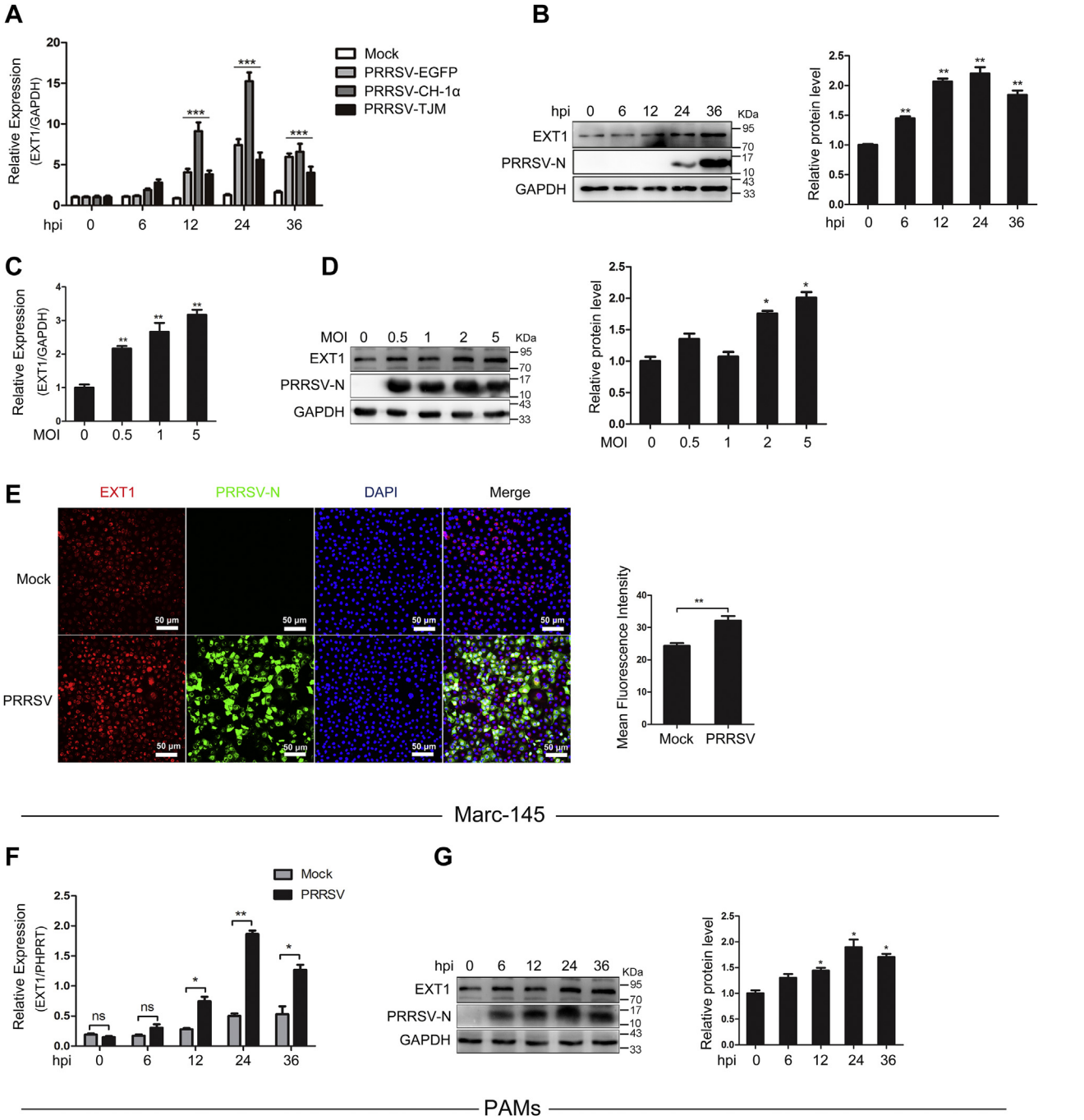

Figure 1. PRRSV infection causes an increase of EXT1 expression *in vitro*. *A*, Marc-145 cells were mock-infected or infected with PRRSV-CH-1a, PRRSV-TJM, PRRSV-EGFP, respectively, at an MOI of 0.5 for different time points, and the cells were harvested to detect the mRNA level of EXT1 by RT–qPCR. *B*, Marc-145 cells were mock-infected or infected with PRRSV-CH-1a at an MOI of 0.5 for different time points, and Western blot analysis was performed to detect the protein level of EXT1. Protein abundance was quantified by ImageJ software. *C* and *D*, Marc-145 cells were mock-infected or infected with PRRSV-CH-1a at different MOIs for 24 h, and the cells were harvested to detect the mRNA and protein levels of EXT1 by RT–qPCR and Western blot analysis. Protein abundance was quantified by ImageJ software. *E*, Marc-145 cells were mock-infected or infected with PRRSV-CH-1a at an MOI of 0.5 for 24 h and then fixed for immunofluorescent staining of EXT1 (*red*) and PRRSV N (*green*). Nucleus (*blue*) was stained with DAPI. The bar represents 50 μm. The mean fluorescence intensity was quantified using the ImageJ software. *F* and *G*, PAMs were mock-infected or infected with PRRSV-CH-1a at an MOI of 0.5 for various time points, and the mRNA and protein levels of EXT1 were detected by RT–qPCR and Western blot. PHPRT, the hypoxanthine phosphoribosyltransferase of *Sus scrofa*, was used as endogenous reference in RT–qPCR. Protein abundance was quantified by ImageJ software. Data are represented as mean ± SE of the three biological replicates. Significant differences are indicated as follows: $*p < 0.05$ and $**p < 0.01$. DAPI, 4′,6-diamidino-2-phenylindole; EGFP, enhanced GFP; EXT1, exostosin glycosyltransferase 1; MOI, multiplicity of infection; PAM, porcine alveolar macrophage; PRRSV, porcine reproductive and respiratory syndrome virus; qPCR, quantitative PCR.

catalytic domain of mouse EXTL2, which uncovered other important residues for the maintenance of transferase activity in addition to the DXD motif, we mutated Asn-651, Asp-654, and Arg-701 of the monkey EXT1 individually or together to alanine (Fig. 4*I*). These three residues mapped to Asn-243, Asp-246, and Arg-293, respectively, of the mouse EXTL2,

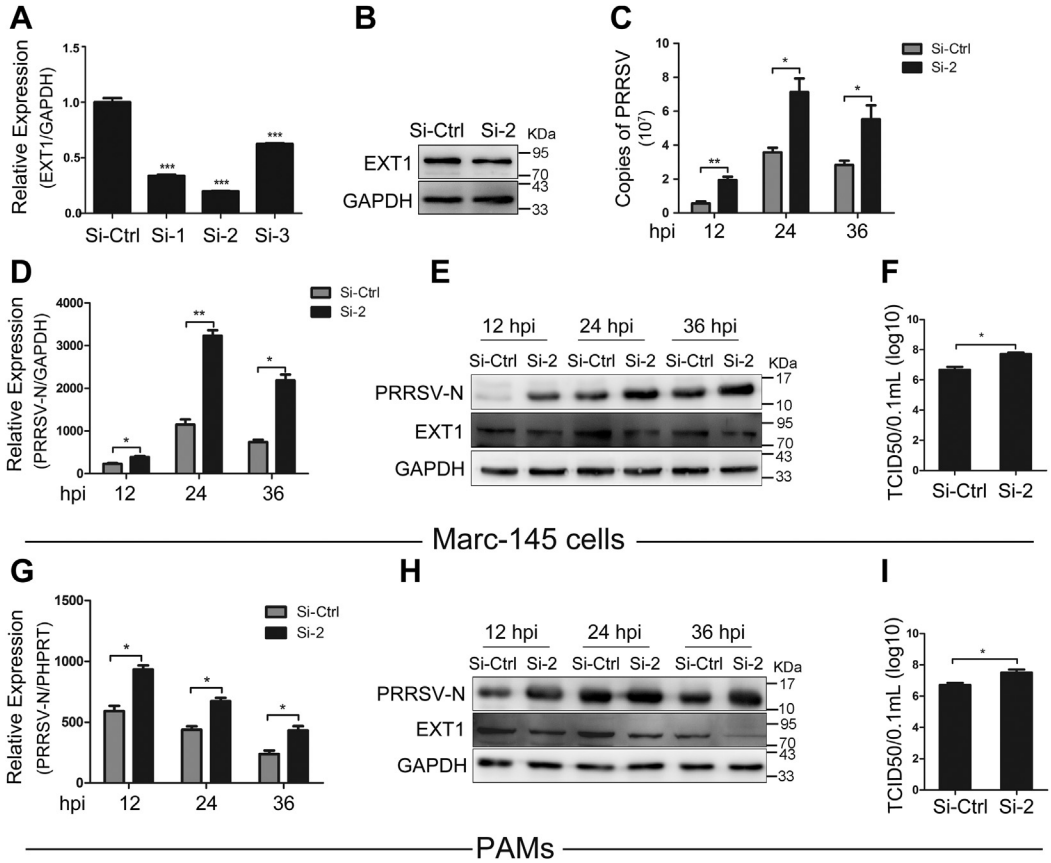

Figure 2. EXT1 knockdown enhances PRRSV infection. *A*, Marc-145 cells were transiently transfected with three independent EXT1-specific siRNAs for 24 h and harvested for RT–qPCR to examine the EXT1 knockdown efficiency. *B*, Western blot analysis to examine the expression of EXT1 protein in EXT1-specific siRNA2-transfected Marc-145 cells. *C*, Marc-145 cells were transiently transfected with EXT1-specific siRNA2 for 24 h and then infected with PRRSV at an MOI of 0.5 for various times. The copy numbers of PRRSV M were detected by absolute RT–qPCR. *D*, *E*, *G*, and *H*, Marc-145 cells (*D* and *E*) or PAMs (*G* and *H*) were transiently transfected with EXT1-specific siRNA2 for 24 h and then infected with PRRSV at an MOI of 0.5 for various times. The mRNA and protein levels of PRRSV N were detected by RT–qPCR and Western blot. PHPRT, the hypoxanthine phosphoribosyltransferase of *Sus scrofa*, was used as endogenous reference in RT–qPCR. *F* and *I*, Marc-145 cells (*F*) or PAMs (*I*) were transiently transfected with EXT1-specific siRNA2 for 24 h before PRRSV infection (MOI = 0.5). Virus titers were quantified by $TCID_{50}$ assay. Data are represented as mean ± SE of the three biological replicates. Significant differences are indicated as follows: $*p < 0.05$, $**p < 0.01$, and $***p < 0.001$. EXT1, exostosin glycosyltransferase 1; MOI, multiplicity of infection; PAM, porcine alveolar macrophage; PRRSV, porcine reproductive and respiratory syndrome virus; qPCR, quantitative PCR; $TCID_{50}$, 50% tissue culture infective dose per milliliter.

which have been proposed as catalytic residues (Fig. 4*I*) (16). We found that overexpression of the ternary mutant EXT1-M6 but not any single mutant (EXT1-M3, EXT1-M4, and EXT1-M5) rescued the restricted PRRSV N induced by EXT1-WT (Fig. 4, *J*–*M*). Taken together, these results indicate that the highly conserved residues Asn-651, Asp-654, and Arg-701 within the glycosyltransferase activity domain of monkey EXT1 may jointly contribute to the inhibition effect on PRRSV.

EXT1 takes part in PRRSV RNA replication but has no effects on viral attachment, internalization, or release

Having demonstrated that EXT1 restricts PRRSV infection, we next examined which stage of the viral life cycle was blocked. Marc-145 cells were transiently transfected with siRNA2 targeting EXT1 for 24 h and incubated with PRRSV virions at an MOI of 10 for 1.5 h at 4 °C allowing for attachment. For the PRRSV internalization, cells were subsequently switched to 37 °C from 4 °C for 1 h after removal of unbound virus. The cells were harvested to detect the level of PRRSV N. EXT1 expression was also determined by RT–qPCR and Western blot analysis (Fig. 5*A*). EXT1 knockdown neither affected the attachment (Fig. 5, *B* and *C*) nor internalization of PRRSV (Fig. 5*D*). As for the role of EXT1 on viral release, cells transfected with siRNA2 were infected with PRRSV at an MOI of 0.5 for 36 h, and we calculated viral release based on intracellular and extracellular viral N levels. EXT1 knockdown did not impair PRRSV release as evaluated by Western blot analysis (Fig. 5*E*). According to these results, we hypothesized that EXT1 may take part in the stage of PRRSV genome replication. As expected, EXT1 knockdown significantly elevated the level of dsRNA, an intermediate in viral genome replication (Fig. 5*F*).

EXT1 mediates PRRSV nsp3 and nsp5 reduction through proteasome degradation pathway

Arterivirus RNA synthesis entails a series of nsps. The restriction of EXT1 on PRRSV RNA replication (Fig. 5*F*) may

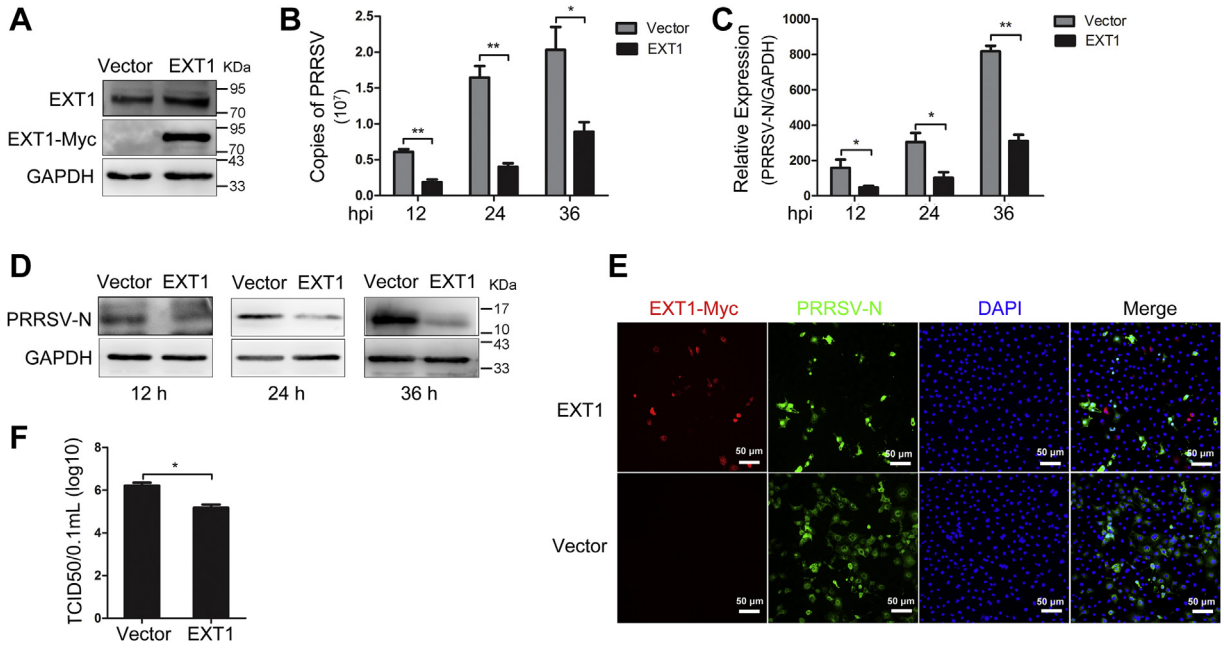

Figure 3. Overexpression of EXT1 inhibits PRRSV infection. *A*, Marc-145 cells were transiently transfected with Myc-tagged EXT1 plasmid or empty vector for 36 h, and EXT1 protein level was determined by Western blot. *B*, Marc-145 cells were transfected with Myc-tagged EXT1 plasmid or empty vector and then infected with PRRSV at an MOI of 0.5 for various times. The copy numbers of PRRSV M were detected by absolute RT–qPCR. *C* and *D*, the mRNA (*C*) and protein levels (*D*) of PRRSV N in Myc-tagged EXT1-transfected Marc-145 cells at various time points. *E*, Marc-145 cells were transfected with Myc-tagged EXT1 plasmid or empty vector for 24 h prior to PRRSV infection (MOI = 0.5). At 24 h postinfection (hpi), cells were fixed for immunofluorescent staining of PRRSV N (*green*) and EXT1-Myc (*red*). And nucleus (*blue*) was stained with DAPI. The bar represents 50 μm. *F*, Marc-145 cells were transiently transfected with Myc-tagged EXT1 plasmid or empty vector for 24 h before PRRSV infection (MOI = 0.5). At 24 hpi, virus titers were quantified by $TCID_{50}$ assay. Data are represented as mean ± SE of the three biological replicates. Significant differences are indicated as follows: $^{*}p < 0.05$ and $^{**}p < 0.01$. DAPI, 4′,6-diamidino-2-phenylindole; EXT1, exostosin glycosyltransferase 1; MOI, multiplicity of infection; PRRSV, porcine reproductive and respiratory syndrome virus; qPCR, quantitative PCR; $TCID_{50}$, 50% tissue culture infective dose per milliliter.

result from impaired viral nsps important for viral replication. To test this, we cotransfected 293T cells with plasmids encoding Myc-tagged monkey EXT1 and each mCherry-tagged PRRSV nsp (nsp1, nsp2, nsp3, nsp4, nsp5, nsp7, nsp8, nsp10, nsp11, or nsp12). All the exogenous proteins were expressed well in 293T cells, and EXT1 expression significantly reduced the protein abundance of PRRSV nsp3 and nsp5 but not of other viral nsps (Fig. 6*A*). We cotransfected 293T cells to express monkey EXT1-D1 and each of these two nsps. We observed that the glycosyltransferase activity domain–deleted EXT1-D1 reversed the inhibitory effect of EXT1-WT on nsp3 and nsp5 (Fig. 6*B*). Next, we used the specific anti-nsp3 antibody (Ab) to detect its protein level in the context of viral infection. Marc-145 cells were transiently transfected with Myc-tagged EXT1-WT or EXT1-D1 for 24 h and then infected with PRRSV for 18 h at an MOI of 1. We found that EXT1-WT but not EXT1-D1 obviously inhibited the viral nsp3 production (Fig. 6*C*). These results suggest that EXT1 inhibits PRRSV nsp3 and nsp5 *via* its glycosyltransferase domain.

Given that all the PRRSV nsps are proteolytic products of the polyproteins, pp1a and pp1ab, and just nsp3 and nsp5 are reduced by EXT1 among these nsps, we reasoned that EXT1 may specifically accelerate the degradation of nsp3 and nsp5. Ubiquitin (Ub)–proteasome system and autophagy–lysosome are two major quality control systems responsible for degradation of proteins and organelles in eukaryotic cells (18). To determine the pathway by which viral nsp3 and nsp5 were degraded induced by EXT1, the proteasome inhibitor MG132 or the lysosomal protease inhibitor leupeptin was added to cells at 24 h after transfection. After 6 h, the cells were harvested for nsp3 or nsp5 examination. MG132 treatment of the Myc-tagged EXT1-transfected cells restored the nsp3 or nsp5 protein to a level comparable to the vector-transfected cells. The level of nsp3 or nsp5 in Myc-tagged EXT1-D1 expressing cells remained similar to that in the vector-expressing cells no matter with or without MG132 (Fig. 6*D*). Consistent with these data, in PRRSV-infected Marc-145 cells, MG132 treatment restored the impaired viral nsp3 induced by EXT1 at the early time point (Fig. 6*E*). However, the level of nsp3 or nsp5 was not rescued by application of leupeptin in Myc-tagged EXT1-transfected 293T cells (Fig. 6*F*). Similarly, in the infected Marc-145 cells, EXT1 overexpression still decreased PRRSV nsp3 even with leupeptin treatment (Fig. 6*G*). These results suggest that EXT1-mediated reduction of nsp3 or nsp5 is dependent on a proteasome degradation pathway, and the C-terminal glycosyltransferase activity domain is responsible for its induced degradation.

EXT1 promotes K48-linked polyubiquitination of nsp3 and nsp5

A recent analysis of the ubiquitome of PRRSV-infected cells has identified 64 ubiquitinated residues on the 15 viral proteins including nsp3 (19). We first determined whether Ub can be

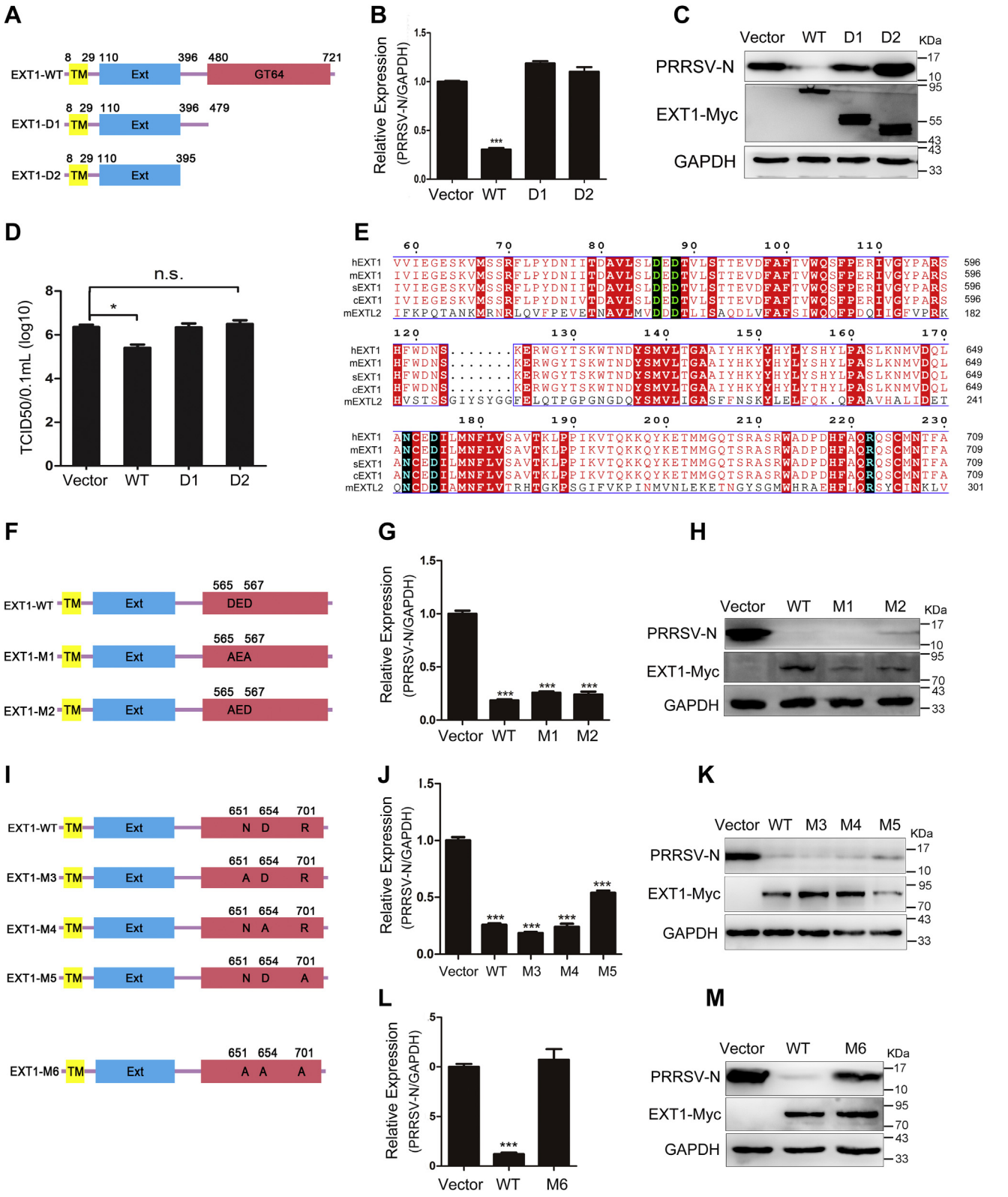

Figure 4. The C-terminal glycosyltransferase activity domain harbors residues responsible for the antiviral function of EXT1. *A*, schematic representations of WT EXT1 and enzyme activity–truncated EXT1. EXT1 consists of an N-terminal cytoplasmic tail, a transmembrane (TM) domain, a stalk (Ext), and a C-terminal large globular domain (GT64) that is likely to harbor glycosyltransferase activity. *B* and *C*, Marc-145 cells transfected with empty vector, EXT1-WT, EXT1-D1, or EXT1-D2 plasmids were infected with PRRSV at an MOI of 0.5. At 24 hpi, RT–qPCR and Western blot were performed to detect the transcription (*B*) and protein levels (*C*) of PRRSV N. *D*, Marc-145 cells were transfected with EXT1-WT, EXT1-D1, EXT1-D2, or empty vector for 24 h before PRRSV infection (MOI = 0.5). Viral titers were quantified by $TCID_{50}$ assay. *E*, amino-acid sequence alignment of the C-terminal activity domain of mEXTL2 and EXT1 from various species. The conserved DXD motif is colored *green*; and the proposed catalytic residues are colored *blue*. hEXT1, the EXT1 of human; mEXT1, the EXT1 of mouse; sEXT1, the EXT1 of pig; cEXT1, the EXT1 of monkey; and mEXTL2, the EXTL2 of mouse. This alignment was created using ClustalW. *F* and *I*, conserved residues for catalysis activity within the C terminus of monkey EXT1 and the cloned mutations. *G*, *H*, *J*, *K*, *L*, and *M*, Marc-145 cells

conjugated to the protein of nsp3 or nsp5. 293T cells were cotransfected plasmids expressing nsp3 or nsp5 along with the hemagglutinin (HA)-tagged monkey Ub. After treatment with MG132, cells were lysed for immunoprecipitation (IP) with anti-mCherry Ab followed by Western blot analysis of Ub using anti-HA Ab. The appearance of smeared higher molecular weight bands in Western blot from the cotransfected cell samples suggested that nsp3 or nsp5 of PRRSV was indeed polyubiquitinated (Fig. 7, *A* and *B*). Furthermore, we investigated the impact of EXT1 on the ubiquitination level of these two viral nsps. 293T cells were cotransfected with plasmids encoding EXT1-WT or EXT1-D1 together with viral nsp3 or nsp5. We found that the ubiquitination level of nsp3 was increased in the presence of EXT1-WT but not changed in the presence of EXT1-D1 (Fig. 7*C*). The similar results were obtained in the nsp5-transfected cells (Fig. 7*D*). These data suggest that EXT1 promotes nsp3 or nsp5 ubiquitination. K48-linked ubiquitination targets substrates for proteasome degradation. By contrast, K63-linked ubiquitination mediates signal transduction. To test which form of EXT1-mediated polyubiquitination of nsp3 or nsp5, Ub mutant plasmids 48K and 63K, which contain arginine substitutions of all its lysine residues except the one at positions 48 and 63, respectively, were used for transfection. We found more K48-linked ubiquitination of nsp3 or nsp5 in the presence of EXT1-WT (Fig. 7, *E* and *F*). However, the amount of K63-linked ubiquitination of these two proteins remained unchanged in the presence of EXT1-WT (Fig. 7, *G* and *H*). Together, the results indicate that EXT1 promotes the K48-linked polyubiquitination of nsp3 or nsp5, thus facilitating their degradation.

EXT1 interacts with PRRSV nsp3 and nsp5 via *its N-terminal cytoplasmic tail*

Next, we investigate the interactions between EXT1 and these two nsps. The confocal microscopy assay demonstrated a significant degree of overlap between Myc-tagged EXT1 and mCherry-tagged nsp3 or nsp5 in 293T cells (Fig. 8*A*). Since EXT1 was located at the ER or Golgi membrane, we further found that the interactions between EXT1 and nsp3 or nsp5 were strikingly colocated with both ER marker calnexin and Golgi marker 58k (Fig. 8*A*). The co-IP results that mCherry-tagged nsp3 or nsp5 but not other viral nsps was coprecipitated with Myc-tagged EXT1 further confirmed this interaction (Fig. 8*B*). Meanwhile, in infected Marc-145 cells, anti-Myc Ab specifically pulled down PRRSV nsp3, further verifying the interaction of EXT1 with viral nsp3 (Fig. 8*C*). To investigate the regions of EXT1 required for its binding to viral nsp3 or nsp5, a series of truncated variants in addition to the EXT1-D1 were generated, including the stalk domain deletion truncation EXT1-D3, the N-terminal cytoplasmic tail deletion truncation EXT1-D4, and the TM domain together with the cytoplasmic tail deletion truncation EXT1-D5 (Fig. 8*D*). The co-IP results revealed that mCherry-tagged nsp3 or nsp5 was pulled down by both Myc-tagged EXT1-D1 and EXT1-D3 (Fig. 8, *E* and *F*). However, neither Myc-tagged EXT1-D4 nor EXT1-D5 could pull down mCherry-tagged nsp3 or nsp5 (Fig. 8, *G* and *H*). These data suggest that EXT1 binds to PRRSV nsp3 and nsp5 *via* its cytoplasmic tail.

EXT1 interacts with EXT2 that inhibits PRRSV infection

Previous studies have reported that EXT2, the other member of the EXT family, forms a hetero-oligomeric complex *in vivo* with EXT1 to cooperatively generate the active enzyme responsible for the polymerization of HS (20). Given the inhibition role of EXT1 on PRRSV, we assessed whether EXT2 conserves the similar function. Exogenous expression of monkey EXT2 in Marc-145 cells significantly diminished the protein level of PRRSV N as shown in Fig. S1*A*, suggesting that homologous EXT2 also acts as a host restriction factor in Marc-145 cells. We next performed immunofluorescence staining and confocal microscopy assays using 293T cells, and results revealed a significant colocalization of the Myc-tagged EXT1 and FLAG-tagged EXT2 (Fig. S1*B*). The co-IP results that anti-Myc Ab effectively pulled down FLAG-tagged EXT2 and the Myc-tagged EXT1 was effectively coimmunoprecipitated with FLAG-tagged EXT2 further corroborated the physical interactions (Fig. S1*C*). Collectively, these data show that the EXT2 protein interacts with EXT1 and may inhibit PRRSV infection *in vitro*.

EXT1 restricts PEAV and PEDV infection in Vero cells

To evaluate whether the antiviral effect of EXT1 is specific to PRRSV, we investigated the effects of EXT1 on PEDV and PEAV, two emerging enteric viruses of swine that belong to order Nidovirales together with PRRSV (21). Vero cells were transiently transfected with siRNA2 targeting EXT1 or Si-Ctrl for 24 h and infected with PEDV and PEAV at an MOI of 0.5 and 0.1, respectively, for various times. We found a higher mRNA level of PEDV or PEAV N in siRNA2-transfected cells compared with that in Si-Ctrl-transfected cells at 12 and 24 hpi (Fig. 9, *A* and *B*). Correspondingly, the N protein levels of these two viruses were also elevated in siRNA2-transfected cells (Fig. 9, *C* and *D*). The immunofluorescence assay of PEDV or PEAV N further demonstrated the phenomenon (Fig. 9, *E* and *F*). Altogether, these data reveal that EXT1 acts as a restriction factor for PEDV and PEAV in Vero cells suggesting for a probable broad-spectrum antiviral function of EXT1.

Discussion

EXT1, as one of the glycosyltransferases, transfers β1,4-linked GlcA and α1,4-linked GlcNAc units alternately

were transfected with Myc-tagged EXT1-WT plasmid or different Myc-tagged EXT1 mutation plasmids for 24 h and then infected with PRRSV at an MOI of 0.5. At 24 hpi, the cells were harvested to detect the PRRSV N transcription (*G*, *J*, and *L*) and protein levels (*H*, *K*, and *M*) by RT–qPCR and Western blot, respectively. Data are represented as mean ± SE of the three biological replicates. Significant differences are indicated as follows: $^{*}p < 0.05$, $^{**}p < 0.01$, and $^{***}p < 0.001$. DXD, aspartic acid–any amino acid–aspartic acid; EXT1, exostosin glycosyltransferase 1; hpi, hours postinfection; MOI, multiplicity of infection; PRRSV, porcine reproductive and respiratory syndrome virus; qPCR, quantitative PCR; $TCID_{50}$, 50% tissue culture infective dose per milliliter.

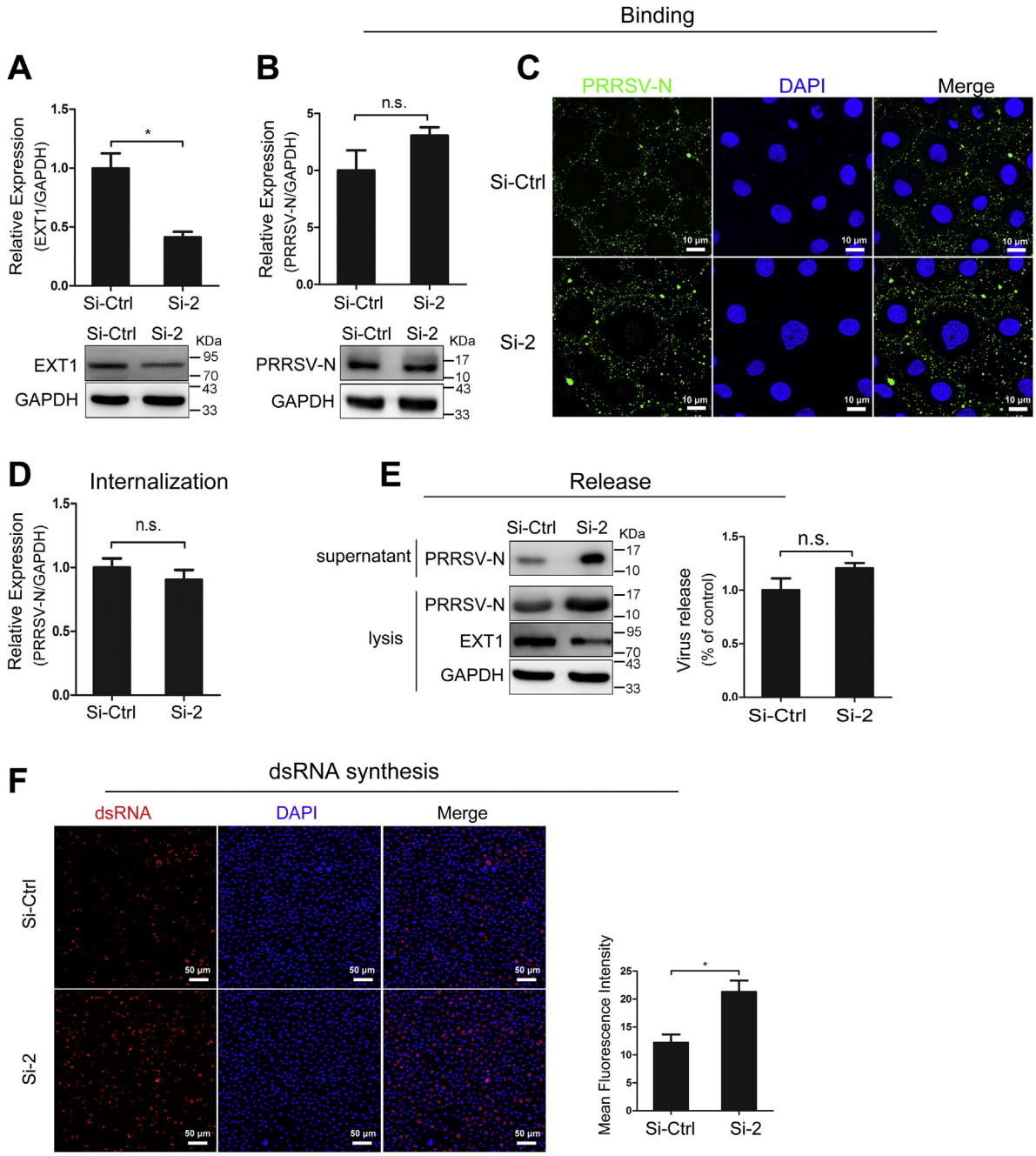

Figure 5. EXT1 takes part in the PRRSV RNA replication but has no effects on viral attachment, internalization, or release. *A*, Marc-145 cells were transiently transfected with siRNA2 for 24 h and harvested for RT–qPCR and Western blot to examine the EXT1 knockdown efficiency. *B–D*, Marc-145 cells transiently transfected with siRNA2 were inoculated with virions at an MOI of 10 for 1.5 h at 4 °C or subsequently switched to 37 °C for 1 h after removal of unbound virus. The bound (*B* and *C*) and internalized (*D*) virions were detected by RT–qPCR, Western blot, or immunofluorescence staining. The bar represents 10 μm. *E*, Marc-145 cells were transiently transfected with siRNA2 for 24 h and infected with PRRSV at an MOI of 0.5 for 36 h. The PRRSV N in cell lysate or supernatant was detected by Western blot and quantified by Image Jsoftware. Viral release efficiency was determined as the ratio of intracellular and extracellular N levels. *F*, Marc-145 cells were transiently transfected with siRNA2 for 24 h and infected with PRRSV at an MOI of 0.5. At 18 hpi, the cells were fixed for immunofluorescent staining of dsRNA (*red*). Nucleus (*blue*) was stained with DAPI. The bar represents 50 μm. The mean fluorescence intensity was quantified using the ImageJ software. Data are represented as mean ± SE of the three biological replicates. Significant differences are indicated as follows: $*p < 0.05$. DAPI, 4′,6-diamidino-2-phenylindole; EXT1, exostosin glycosyltransferase 1; hpi, hours postinfection; MOI, multiplicity of infection; PRRSV, porcine reproductive and respiratory syndrome virus; qPCR, quantitative PCR.

from the respective UDP-sugars to the nonreducing end of the growing HS polymer during the process of HS biosynthesis (8). EXT1 defect or mutation not only impairs the mount of HS but also affects HS structure (17, 22). Recently, EXT1 protein has been screened out as an essential host factor for several viruses by the technique of genome-wide CRISPR–Cas9 screen, including severe acute respiratory syndrome respiratory syndrome coronavirus 2, dengue virus, Zika virus, and Japanese encephalitis virus (11–13). It has been reported that EXT1 knockdown weakened the entry process of Marburg virus (10). The primary infection of vaccinia virus was reduced in EXT1 knockout cells because

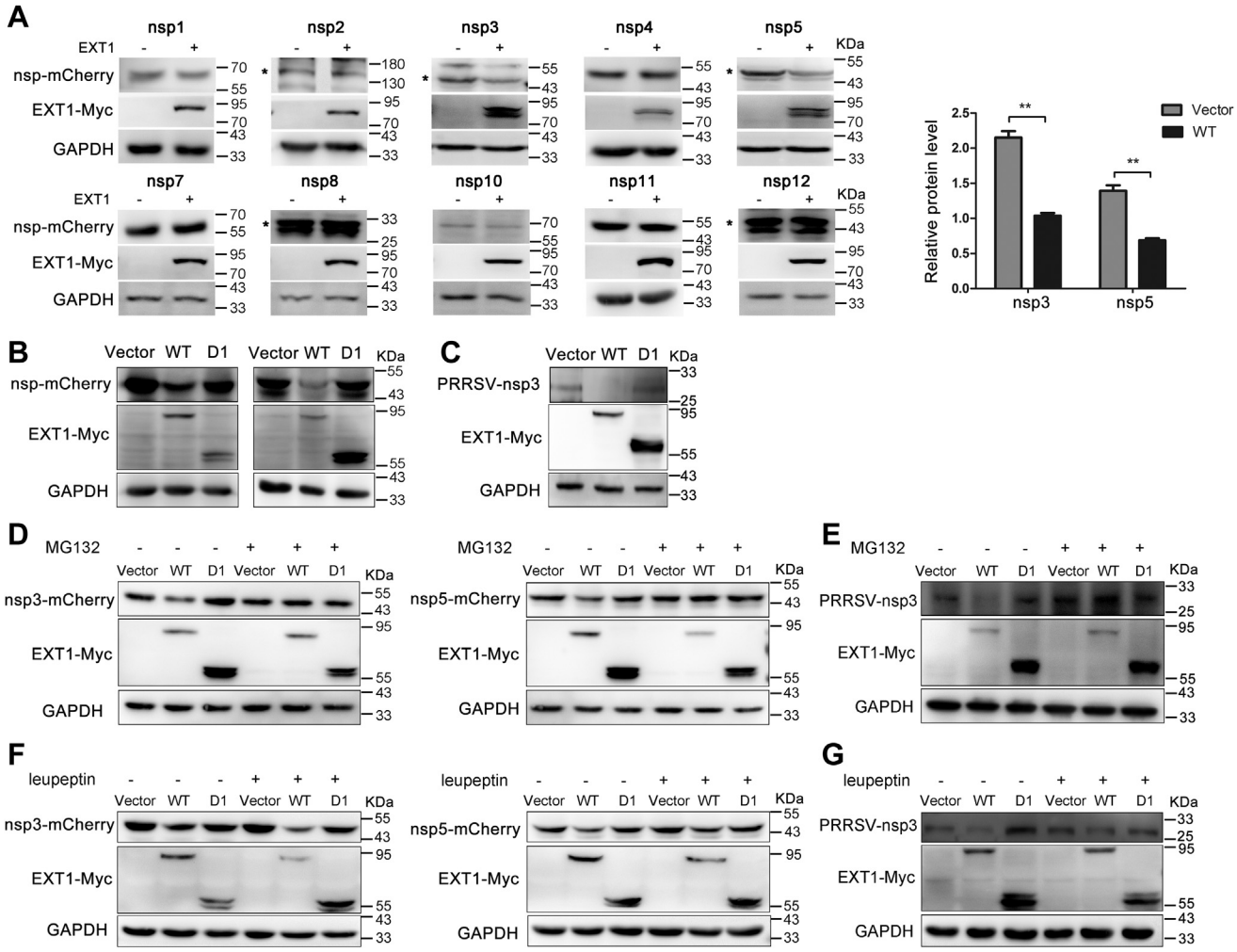

Figure 6. EXT1 mediates PRRSV nsp3 and nsp5 reduction through proteasome degradation. *A* and *B*, 293T cells were cotransfected with Myc-tagged EXT1-WT or EXT1-D1 along with different mCherry-tagged PRRSV nsp-expressing plasmids, and 36 h later, cells were lysed for Western blot to analyze the abundance of PRRSV nsps. The abundance of PRRSV nsp3 and nsp5 in *A* was quantified by ImageJ software. The *asterisks* indicate the specific nsp protein bands. *C*, Marc-145 cells were transiently transfected with Myc-tagged EXT1-WT or EXT1-D1 plasmid for 36 h and then infected with PRRSV at an MOI of 1 for 18 h. The cells were lysed for Western blot to examine PRRSV nsp3. *D*, 293T cells were cotransfected with Myc-tagged EXT1-WT or EXT1-D1 together with mCherry-tagged PRRSV nsp3- or nsp5-expressing plasmids; 24 h later, cells were treated with MG132 (10 μM) for another 6 h and harvested to detect the nsp3 (*left*) or nsp5 (*right*) protein level. *E*, Myc-tagged EXT1-WT- or EXT1-D1-transfected Marc-145 cells were infected with PRRSV for 12 h at an MOI of 1 and then treated with MG132 (10 μM) for 6 h. The cells were lysed for Western blot using antibody against PRRSV nsp3. *F*, 293T cells were cotransfected with Myc-tagged EXT1-WT or EXT1-D1 and mCherry-tagged PRRSV nsp3- or nsp5-expressing plasmids for 24 h and treated with leupeptin (200 μM) for another 6 h. Cells were harvested to determine the nsp3 (*left*) or nsp5 (*right*) protein level. *G*, Myc-tagged EXT1-WT- or EXT1-D1-transfected Marc-145 cells were infected with PRRSV at an MOI of 1 for 12 h and then treated with leupeptin (200 μM) for 6 h. The cells were lysed for Western blot using antibody against PRRSV nsp3. EXT1, exostosin glycosyltransferase 1; MOI, multiplicity of infection; nsp, nonstructural protein; PRRSV, porcine reproductive and respiratory syndrome virus.

the synthesis of HS was blocked (14). These instances suggest that EXT1 plays as a proviral factor. However, orthogonal genome-wide screening identified EXT1 as a host restriction factor for influenza A virus in bat cells (23). Similar to influenza A virus, the results presented here reveal an antiviral role of EXT1 in PRRSV infection (Figs. 2, *C–I* and 3, *B–F*). EXT1 knockdown in Marc-145 cells enhanced PRRSV RNA replication but had no effects on the initial virus binding, entry, or later release (Fig. 5, *B–F*). For these results, we consider that the restriction role of EXT1 on PRRSV replication is unlikely associated with HS. What is more, we found that the restrained role of EXT1 is not specific to PRRSV. EXT1 also inhibited the infection of PEDV and PEAV, two swine enteric viruses that belong to order Nidovirales together with PRRSV (Fig. 9). These results suggest that EXT1 may play a broad-spectrum antiviral function.

Although the C-terminal part of EXT1 has been identified as the catalytic activity domain, the exact sites involved in this catalytic function remain unclear. The solved X-ray crystal structure of the catalytic domain of mouse EXTL2 provides us an excellent model for investigating the structure-based mechanism of the transferase reaction catalyzed by the EXT gene family (16). The Asn-243, Asp-246, and Arg-293 within the mouse EXTL2 have been reported to locate at the active site. The Asp-246 is proposed as catalytic residue, and the Arg-293 interacts with the donor sugar of UDP-GlcNAc. These three residues have been predicted to work together to orient the substrates in the proper position for catalysis. The

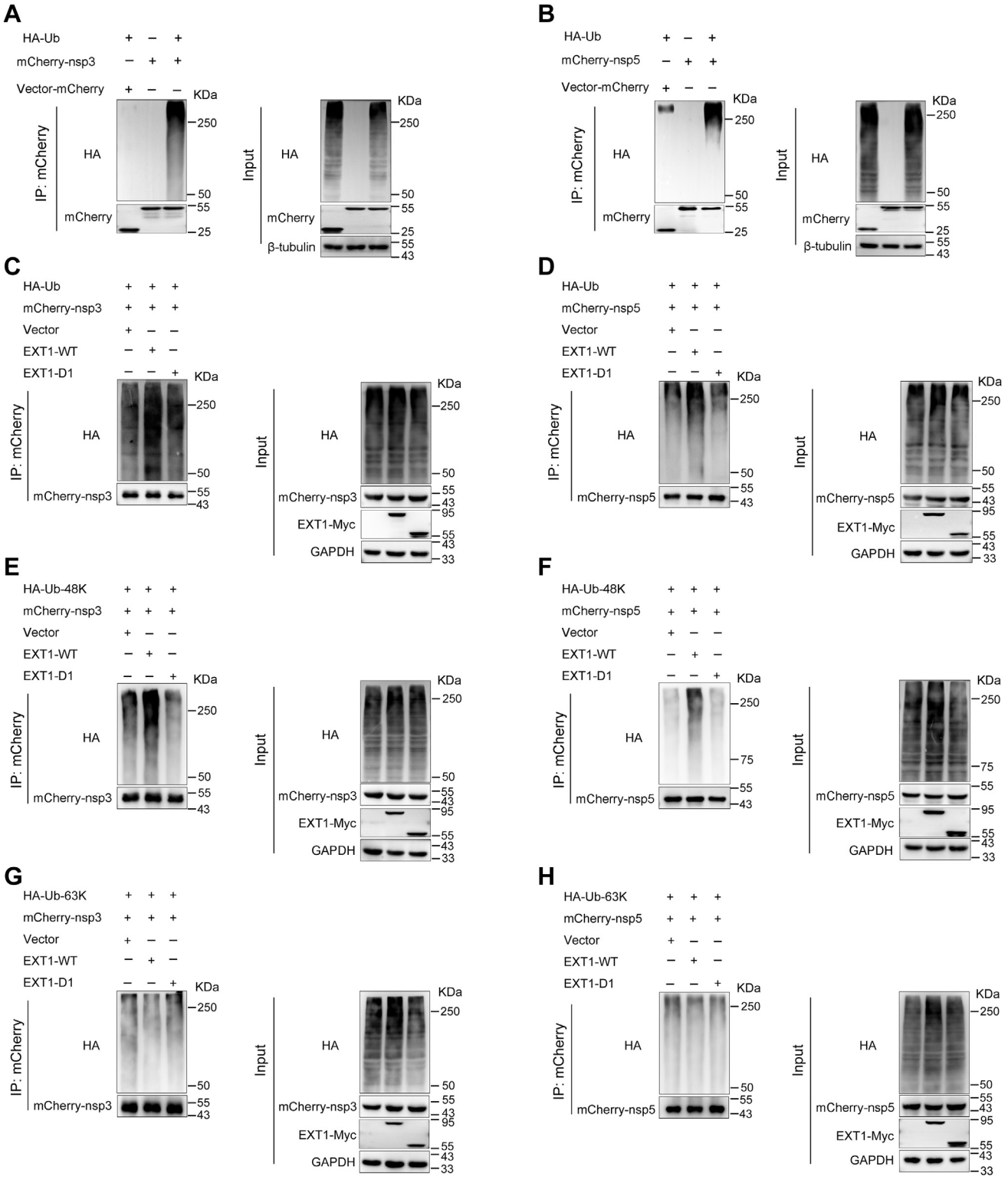

Figure 7. EXT1 promotes K48-linked polyubiquitination of nsp3 and nsp5. *A* and *B*, 293T cells were cotransfected with mCherry-tagged nsp3 or nsp5 together with HA-tagged ubiquitin for 24 h and were treated with MG132 (10 μM) for another 6 h. Then the cells were lysed for coimmunoprecipitation (co-IP) using an antibody against mCherry. The immunoprecipitates were analyzed by Western blot with antibodies against HA and mCherry. *C* and *D*, co-IP and Western blot analysis of 293T cells transfected with various combinations of plasmids encoding Myc-tagged EXT1-WT, Myc-tagged EXT1-D1, mCherry-tagged nsp3 (*C*) or nsp5 (*D*), and HA-tagged ubiquitin and treated with MG132 (10 μM). *E* and *G*, co-IP and Western blot analysis of 293T cells transfected with various combinations of plasmids encoding Myc-tagged EXT1-WT, Myc-tagged EXT1-D1, mCherry-tagged nsp3 and HA-tagged K48-linked (*E*) or K63-linked (*G*) ubiquitin, and treated with MG132 (10 μM). *F* and *H*, co-IP and Western blot analysis of 293T cells transfected with various combinations of plasmids encoding Myc-tagged EXT1-WT, Myc-tagged EXT1-D1, mCherry-tagged nsp5 and HA-tagged K48-linked (*F*) or K63-linked (*H*) ubiquitin, and treated with MG132 (10 μM). EXT1, exostosin glycosyltransferase 1; HA, hemagglutinin; nsp, nonstructural protein.

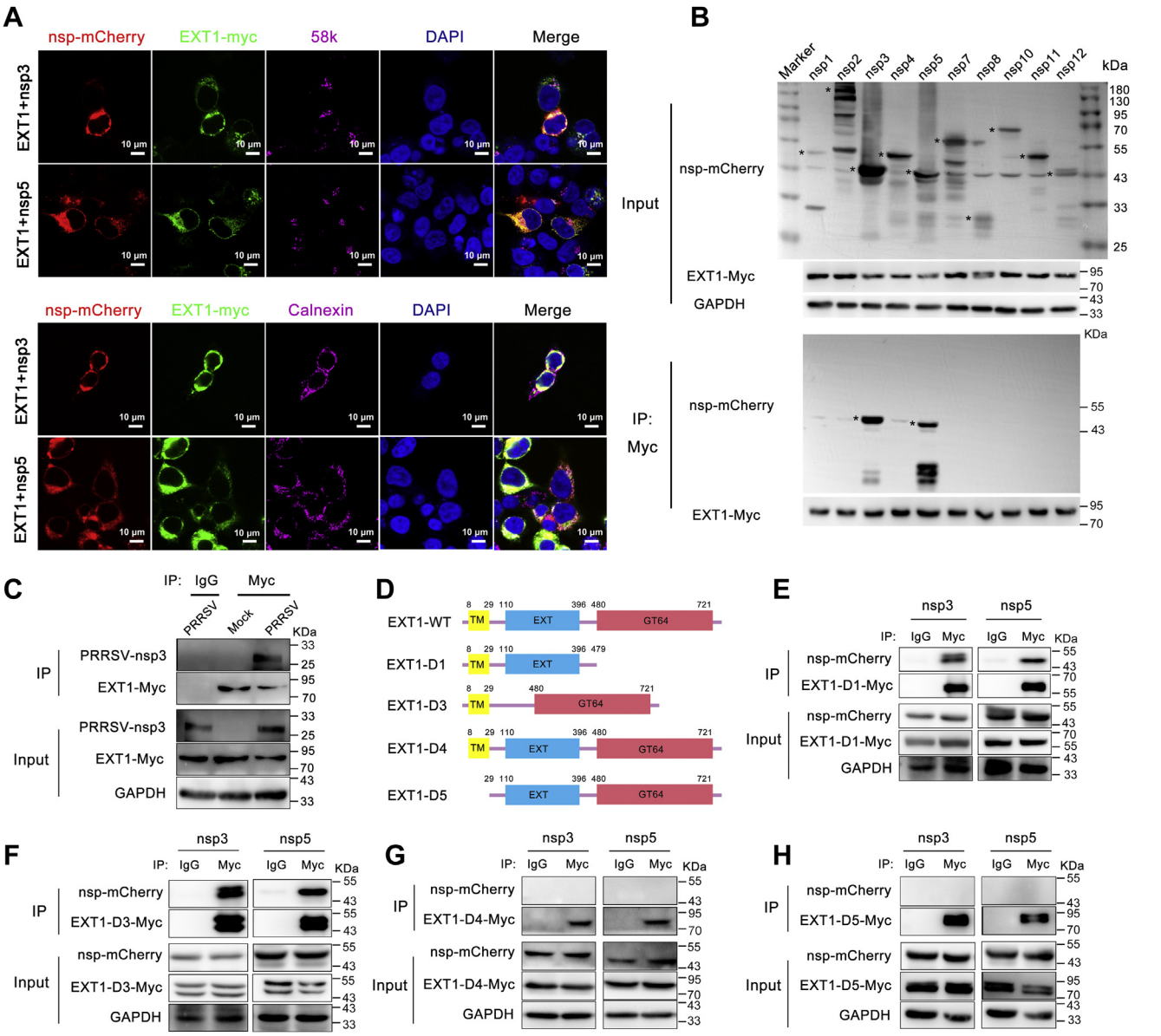

Figure 8. EXT1 interacts with PRRSV nsp3 and nsp5 *via* its N-terminal cytoplasmic tail. *A*, colocalization of EXT1 protein with PRRSV nsp3 or nsp5 in 293T cells. 293T cells were cotransfected with Myc-tagged EXT1 and mCherry-tagged nsp3 or nsp5; 36 h later, the cells were fixed for immunofluorescent staining of EXT1-Myc (*green*), mCherry-nsp3 or nsp5 (*red*), and Golgi marker 58k or ER marker calnexin (*purple*). Nuclei were stained with DAPI (*blue*). Images of cells were acquired by laser-scanning fluorescent confocal microscopy. The bar represents 10 μm. *B*, 293T cells were cotransfected with Myc-tagged EXT1 and different mCherry-tagged PRRSV nsp-expressing plasmids, and 36 h later, cells were lysed for IP to analyze the interactions between EXT1 and these nsps. The *asterisks* indicate the specific nsp protein bands. *C*, Marc-145 cells were transiently transfected with Myc-tagged EXT1 plasmid for 36 h and then infected with PRRSV at an MOI of 0.5. The cells were lysed for IP to detect the interaction between EXT1 and nsp3. *D*, schematic representations of full-length or truncated EXT1. *E–H*, 293T cells were transiently cotransfected with plasmids expressing different EXT1 truncations and nsp3 or nsp5; 36 h later, cells were lysed and subjected to IP using a mouse anti-Myc monoclonal antibody. Immunoprecipitates were analyzed by Western blot with the indicated antibodies. DAPI, 4′,6-diamidino-2-phenylindole; ER, endoplasmic reticulum; EXT1, exostosin glycosyltransferase 1; IP, immunoprecipitation; nsp, nonstructural protein; PRRSV, porcine reproductive and respiratory syndrome virus.

Asn-243, Asp-246, and Arg-293 of the mouse EXTL2 are, respectively, mapped to Asn-651, Asp-654, and Arg-701 of monkey EXT1. We found that only the ternary mutant of EXT1 failed to inhibit PRRSV infection, and all the single mutants kept the restriction role of EXT1 (Fig. 4, *I–M*). These results suggest that Asn-651, Asp-654, and Arg-701 of EXT1 may together contribute to its inhibition of PRRSV. However, whether these three residues of monkey EXT1 possess the glycosyltransferase activity needs to be confirmed further using reliable detection method.

Following PRRSV entry and release of the genome into cytoplasm, the viral life cycle starts with the expression of nsps. PRRSV genome encodes 14 nsps, which exhibit replicase, protease, and polymerase activities and perform essential roles in viral replication (24). Most of these nsps, together with some host cellular factors, are assembled into the membrane-associated viral RTC that anchors to the intracellular membranes to form double-membrane vesicles (DMVs) (3, 25). It is the DMVs that provide a favorable environment for viral replication. The results of this study have shown that the

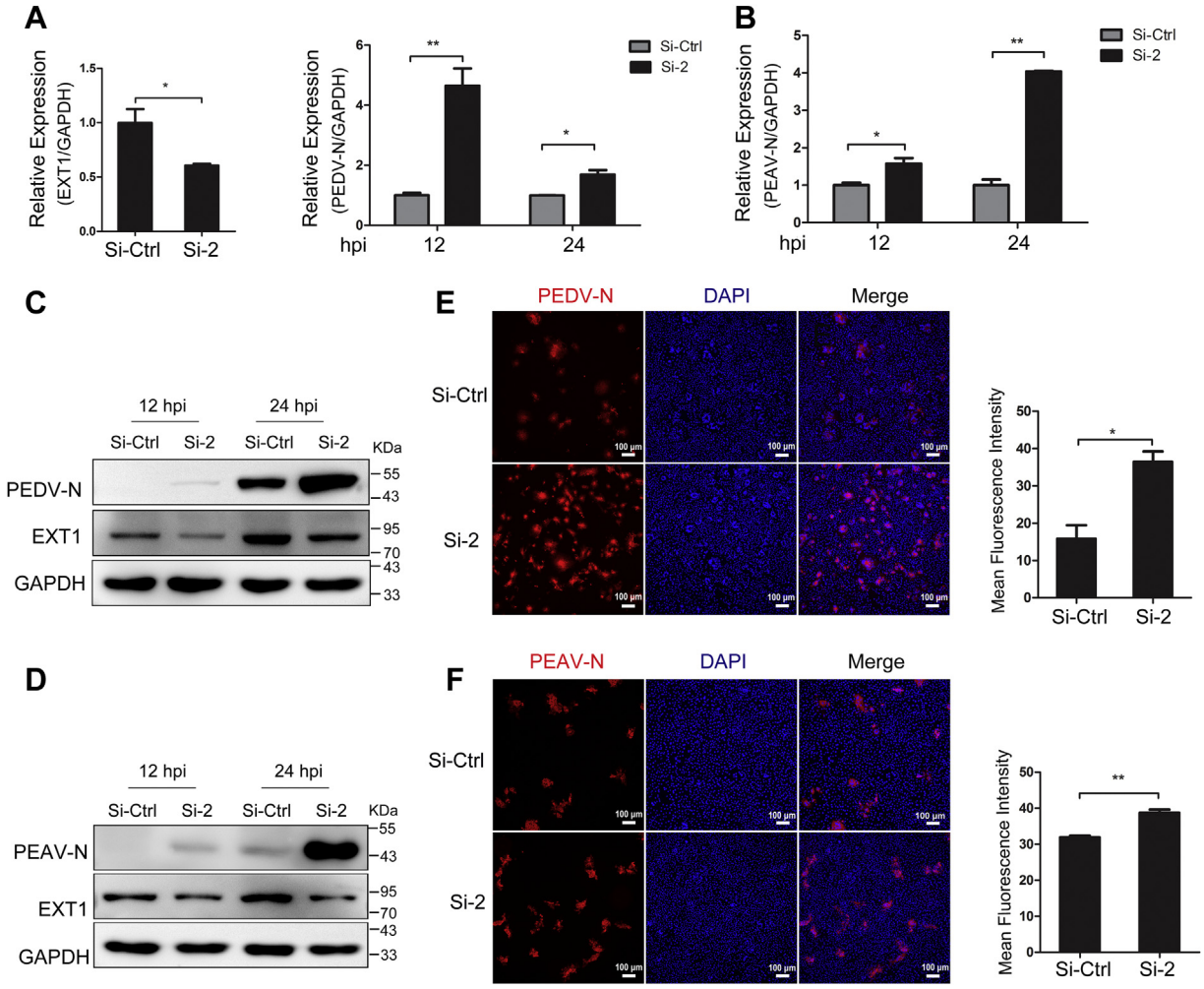

Figure 9. EXT1 restricts PEAV and PEDV infection in Vero cells. *A–D*, Vero cells were transiently transfected with EXT1-specific siRNA2 for 24 h and infected with PEDV (MOI = 0.5) or PEAV (MOI = 0.1) for 12 or 24 h. The cells were harvested for RT–qPCR to determine the mRNA and protein levels of PEDV N (*A* and *C*) or PEAV N (*B* and *D*). The EXT1 knockdown efficiency was also examined. *E* and *F*, Vero cells were transiently transfected with siRNA2 for 24 h and infected with PEDV (MOI = 0.5) or PEAV (MOI = 0.1) for 24 h. The cells were fixed for immunofluorescent staining of PEDV N (*E*) or PEAV N (*F*) (*red*). Nucleus (*blue*) was stained with DAPI. The bar represents 100 μm. The mean fluorescence intensity was quantified using the ImageJ software. Data are represented as mean ± SE of the three biological replicates. Significant differences are indicated as follows: $^{**}p < 0.01$. DAPI, 4′,6-diamidino-2-phenylindole; EXT1, exostosin glycosyltransferase 1; MOI, multiplicity of infection; PEAV, porcine enteric alphacoronavirus; PEDV, porcine epidemic diarrhea virus; qPCR, quantitative PCR.

reduced PRRSV replication induced by EXT1 resulted from Ub–proteasome degradation of viral nsp3 and nsp5 (Figs. 6 and 7). Ub proteasome pathway is important for the degradation of intracellular proteins and can regulate the physiological balance of eukaryotic cell organisms (26). The nsp3 and nsp5 of PRRSV have been reported to possess Ub-binding activity (19, 27). In our study, we confirmed that these two nsps were indeed modified by Ub (Fig. 7, *A* and *B*). And overexpression of EXT1 enhanced the amount of K48-linked polyubiquitination of these two proteins but not K63-linked polyubiquitination (Fig. 7, *C–F*).

The TM proteins nsp3 and nsp5 of PRRSV are thought to be involved in membrane modification and the formation of DMVs (3). Furthermore, the DMVs were derived from ER (28), which provided the possibility for EXT1 to interact with nsp3 and nsp5. We confirmed that nsp3 and nsp5 interacted with EXT1, and the interaction was located at ER or Golgi membrane (Fig. 8, *A–C*). And the cytoplasmic tail of EXT1 was responsible for the binding to nsp3 and nsp5 (Fig. 8, *D–H*). Because of a lack of available Ab specific to PRRSV nsp5, in this study, we just verified the interplay between EXT1 and nsp3 in infected cells, and the effects of EXT1 on PRRSV nsp5 need to be further verified under the context of infection. Since EXT1 was not an E3 Ub ligase, we reasoned that EXT1 might function as an adaptor to recruit an E3 Ub ligase to nsp3 or nsp5. The detailed events that EXT1 regulates ubiquitination level need to be further investigated.

The EXT2 protein, homologous to EXT1, has been shown to do not possess significant HS polymerase activity in the absence of EXT1. Nevertheless, when the EXT1 was overexpressed, accompanied by the overexpression of EXT2, the EXT1-deficient sog9 cells exhibited much higher HS polymerase activity than the case that EXT1 was overexpressed alone (20). What is more, EXT1 and EXT2 form a hetero-oligomeric complex that accumulates in the Golgi (29), where the biosynthesis of HS chains is thought to occur

(30–32). These results support a model in which EXT1 works in concert with EXT2 to provide the HS polymerase activity in the cells. In this study, we tested the interaction between the EXT1 and EXT2 in 293T cells and found that EXT2 also inhibited the PRRSV infection (Fig. S1). Because cell line-deficient EXT1 or EXT2 are not available, we cannot confirm whether EXT2 is involved in the PRRSV inhibition function of EXT1. Likewise, the query whether the EXT1 protein participates in the antiviral function of EXT2 is unknown. This becomes an interesting area for future research.

From our known results, we put forward a possible mechanism of the antiviral function of EXT1 (Fig. 10). PRRSV infection stimulates the expression of EXT1 protein. The EXT1 protein interacts with viral nsp3 and nsp5 *via* its cytoplasmic tail and accelerates the Ub–proteasome degradation of these two nsps. Reduced nsp3 and nsp5 may restrict the formation of viral RTC. The impaired RTC hinders viral RNA replication finally. Our work demonstrates for the first time that EXT1 is an efficient cell-intrinsic antiviral factor against PRRSV infection. These findings should help understand the host antiviral response to PRRSV infection.

Experimental procedures

Ethics statement

The PAMs used in this study were from 6-week-old PRRSV-negative piglets. Animals were euthanized, and carcasses were treated innocuously. The work was approved by the Institutional Animal Care and Use Committee of Sun Yat-sen University.

Cells and viruses

African green monkey kidney cells (Marc-145 and Vero cells) and human embryonic kidney 293T cells were cultured in Dulbecco's modified Eagle's medium (Invitrogen) supplemented with 10% fetal bovine serum (Gibco) and incubated at 37 °C in an incubator with 5% CO_2. PAMs were isolated from lung lavage samples of the 6-week-old PRRSV-negative piglets (33, 34) and cultured in RPMI1640 medium supplemented with 10% fetal bovine serum (Gibco), 100 U/ml penicillin, and 100 mg/ml streptomycin at 37 °C in 5% CO_2. Two PRRSV-2 strains, CH-1a (GenBank accession number: AY032626.1) and TJM (GenBank accession number: MG972945.1) were kindly offered by Dr Guihong Zhang of South China Agricultural University. A recombinant PRRSV strain, PRRSV-EGFP, was gifted from Dr Shuqi Xiao of Northwest A&F University, China. The EGFP was inserted between the N protein and 3′-UTR of the PRRSV genome (35). All the PRRSV strains were propagated and titrated on Marc-145 cells. If not clearly indicated, the PRRSV strain used in the study was PRRSV-CH-1a. PEDV strain GDS01 (GenBank accession number: KM089829.1) and PEAV strain GDS04 (GenBank accession number: MH697599.1) were gifted from Dr Yongchang Cao of Sun Yat-sen University, China.

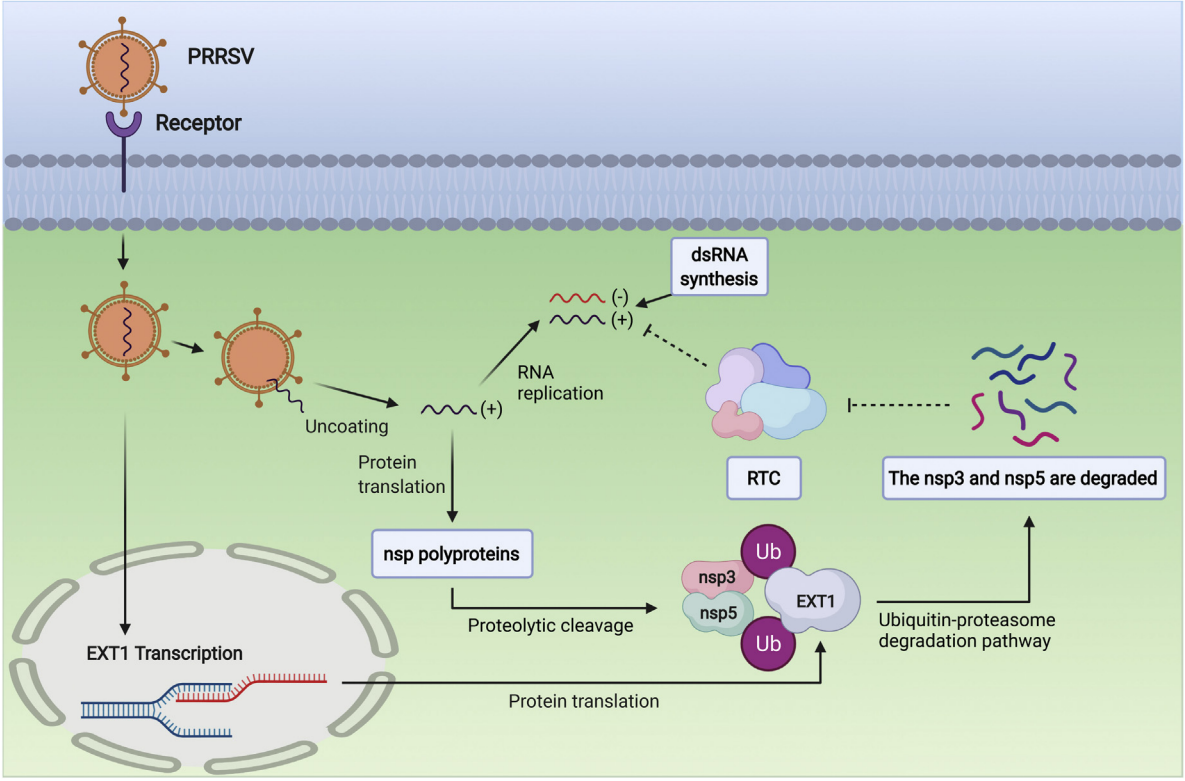

Figure 10. Schematic model of EXT1 regulation of PRRSV infection. PRRSV infection induces the expression of EXT1, which displays an anti-PRRSV activity. EXT1 interacts with viral nsp3 and nsp5 *via* its cytoplasmic tail and accelerates the K48-linked ubiquitination of these two nsps, resulting in their degradation. The reduced nsp3 and nsp5 restricts the formation of viral RTC, impairing the viral dsRNA synthesis. EXT1, exostosin glycosyltransferase 1; nsp, nonstructural protein; PRRSV, porcine reproductive and respiratory syndrome virus; RTC, replication transcription complex.

RT–qPCR

Total RNA was isolated from Marc-145 cells using TRIzol reagent (Invitrogen) and then reverse transcribed into complementary DNA with a GoScript RT Reagent Kit (Promega) according to the manufacturer's instructions. To quantify the mRNA levels of EXT1 and PRRSV N, relative RT–qPCR was performed using a Light-Cycler 480 PCR system (Roche). The expression levels of target genes were normalized to the endogenous reference gene GAPDH using the $2^{-\Delta\Delta Ct}$ method (where Ct is the threshold cycle). For the virus copies in infected Marc-145 cells, absolute RT–qPCR was conducted to quantify PRRSV M gene expression, and a standard curve was generated using a serially diluted plasmid containing the PRRSV M gene. The primers and TaqMan probe used for RT–qPCR are listed in Table S1.

Western blot analysis

For immunoblotting, Marc-145 cells cultured in 6-well plates were washed twice with cold PBS and lysed in radioimmunoprecipitation assay (RIPA) buffer (Beyotime) containing the proteinase inhibitor, 20 nM PMSF (Sigma). Cell lysates were denatured in 5× SDS-PAGE sample buffer (Beyotime) at 95 °C for 10 min and then subjected to SDS-PAGE. The separated proteins were transferred to the polyvinylidene difluoride membranes (Millipore). The membranes were blocked in 5% bovine serum albumin in TBS with 0.1% Tween-20 for 1 h at room temperature and incubated with a primary Ab overnight at 4 °C. Following three washes in TBS with Tween-20, membranes were incubated with horseradish peroxidase (HRP)–conjugated secondary Abs for 1 h at room temperature. Washed three times again, protein bands were visualized using an enhanced chemiluminescence Kit (FD). Abs used in Western blot analysis: anti-EXT1 (1:1000 dilution; catalog no.: ab171817; Abcam), anti-PRRSV N (4A5) (1:3000 dilution; catalog no.: 9041; Jeno Biotech), anti-PRRSV nsp3 (1:500 dilution, gifted from Dr Hanchun Yang of China Agricultural University), anti-PEDV N polyclonal Ab (1:1000 dilution; gifted from Dr Yongchang Cao of Sun Yat-sen University), anti-PEAV N polyclonal Ab (1:1000 dilution; gifted from Dr Yongchang Cao of Sun Yat-sen University), anti-GAPDH (1:3000 dilution; catalog no.: GTX100118; GeneTex), anti-β-tubulin (Cell Signaling Technology; 1:2000 dilution; catalog no.: 2146S), anti-Myc (Cell Signaling Technology; 1:2000 dilution; catalog no.: 2276S), anti-mCherry (Abcam; 1:3000 dilution; catalog no.: ab183628), anti-HA (Cell Signaling Technology; 1:2000 dilution; catalog no.: 3724S), anti-FLAG (Cell Signaling Technology; 1:2000 dilution; catalog no.: 14793S), HRP-linked antimouse IgG (Cell Signaling Technology; 1:2000 dilution; catalog no.: 7076), and HRP-linked anti-rabbit IgG (Cell Signaling Technology; 1:2000 dilution; catalog no.: 7074).

Co-IP

Anti-Myc, anti-FLAG, or anti-mCherry Ab–conjugated magnetic beads were first prepared according to the instructions from Dynabeads Protein G Immunoprecipitation Kit (Invitrogen) before IP. Then cells in 6-well plates were washed twice with cold PBS and harvested in RIPA lysis buffer supplemented with 20 nM PMSF and lysed for 30 min on ice. The cell lysates were centrifuged at 12,000*g* at 4 °C for 10 min; supernatants were subjected to IP with anti-Myc, anti-FLAG, or anti-mCherry Ab-conjugated magnetic beads for 2 h at room temperature. Magnetically isolated beads and bound proteins were subsequently washed three times in 200 μl washing buffer; bound proteins were eluted by addition of 20 μl elution buffer with 5 μl 5× SDS-PAGE sample buffer at 95 °C for 10 min. The final samples were separated by SDS-PAGE, and Western blot was performed as described previously.

Immunofluorescence microscopy

Cells were plated on coverslips and then fixed with 4% paraformaldehyde (Beyotime) for 10 min, permeabilized in 0.3% Triton X-100 (Beyotime) in PBS for 5 min, and rinsed with PBS three times. Subsequently, the cells were blocked in PBS with 3% BSA for 30 min and incubated with primary Abs: anti-Myc (Cell Signaling Technology; 1:800 dilution; catalog no.: 2276S), anti-FLAG (1:800 dilution; catalog no.: 14793S; Cell Signaling Technology), anticalnexin (AF18) (1:300 dilution; catalog no.: sc-23954; Santa Cruz Biotechnology), anti-58k Golgi (1:300 dilution; catalog no.: ab27043; Abcam), anti-PEDV N monoclonal Ab (1:1000, gifted from Dr Yongchang Cao of Sun Yat-sen University), anti-PEAV N monoclonal Ab (1:1000; gifted from Dr Yongchang Cao of Sun Yat-sen University), and anti-dsRNA (J2) (1:1000 dilution; catalog no.: 10010200; Scicons,) overnight at 4 °C. After washing three times, cells were incubated with appropriate secondary Abs conjugated to Alexa Fluor 488, 555, or 647 fluorochromes (1:500 dilution; Cell Signaling Technology) at room temperature for 1 h. Cells were washed again then stained with 4′,6-diamidino-2-phenylindole (1:1000 dilution; Beyotime) for 5 min. Finally, images of cells were acquired by an inverted fluorescence microscope (NIKON ECLIPSE Ti2-U) or a confocal laser scanning microscope (TCS-SP5; LEICA).

siRNA knockdown

For transient EXT1 knockdown, the siRNAs used for Marc-145 cells or PAMs were synthesized by Sangon Biotech and had the following sequences: EXT1, siRNA-1, 5′-GCUUCAAAGUCUACGUAUATT-3′; siRNA-2, 5′-CCUUAUAUCACGUCCAUAATT-3′; siRNA-3, 5′-CCAGCUGGUUUGGCUACAUTT-3′, and the corresponding control siRNA, 5′-UUCAAUAAAUUCUUGAGGU-3′. Marc-145 cells or PAM cells were plated on 6-well plates to 70% confluence and then transfected with siRNA-1, siRNA-2, or siRNA-3 at a final concentration of 50 nmol/l using Lipofectamine RNAiMAX Transfection Reagent (Invitrogen) following the manufacturer's instructions. At 36 h post-transfection, cells were collected for RT–qPCR or Western blot analysis to evaluate the knockdown efficiency.

Plasmids and transfection

To construct the green monkey EXT1 or EXT2 expression plasmid, the full-length EXT1 or EXT2 coding sequence was amplified by PCR and then, respectively, inserted into pcDNA3.1(+) M-Myc-C vector (Invitrogen) or pcDNA3.1(+) M-FLAG-C vector (Invitrogen). The truncations and mutations of EXT1-Myc were subcloned from the pcDNA-EXT1 plasmid. Genes of PRRSV nsps were cloned into the pmCherry-N1 vector (Promega) to generate the PRRSV nsp plasmids. Amplification primers used are listed in Table S1. Gene of green monkey Ub B was cloned into the pCMV-HA-N (Promega) to generate the HA-Ub plasmid. The Ub mutant plasmids 48K and 63K were conducted by company of IGEbio. The Marc-145 or 293T cells cultured in 6-well plates were transfected with expression plasmids using Lipofectamine 3000 (Invitrogen) according to the manufacturer's instructions.

PRRSV binding, entry, and release assays

Transfected Marc-145 cells were precooled for 1 h at 4 °C and inoculated with virions at an MOI of 10 for 1.5 h at 4 °C, allowing for viral attachment without internalization. The cells were then washed with cold PBS three times so that unbound viruses were removed. For entry assay, the cells were supplemented with fresh serum-free medium and subsequently shifted to 37 °C for 1 h, allowing virus internalization. The cells were washed with citrate buffer solution (pH 3.0) to remove the noninternalized visions and washed with PBS three times. PRRSV N abundance was determined by RT–qPCR or Western blot. For release assay, the transfected Marc-145 cells were infected with PRRSV at an MOI of 0.5 for 36 h, and then the cells and cell supernatant were collected to extract proteins using RIPA buffer and trichloroacetic acid–acetone, respectively. The PRRSV N protein in the cell lysate or supernatant was detected by Western blot, and viral release efficiency was determined as the ratio of intracellular and extracellular N levels.

Tissue culture infective dose assay of 50%

The titers of virus in the supernatants were determined using a microtitration infectivity assay and expressed as 50% tissue culture infective dose per milliliter. Briefly, the confluent monolayers of Marc-145 cells cultured in 96-well plates were incubated with 10-fold serially diluted virus suspensions for 48 to 60 h, and then the cytopathic effect was recorded. Virus titers were determined by the method of Reed–Muench.

Statistical analysis

All the data were presented as means ± SE. Samples' values were analyzed using a two-tailed unpaired Student's t test for two groups and ANOVA for multiple comparisons. Significance levels are $^{*}p < 0.05$, $^{**}p < 0.01$, and $^{***}p < 0.001$. All cellular experiments were repeated at least three times. Statistical analysis was performed in GraphPad Prism (GraphPad Software, Inc).

Data availability

All data are contained within the article.

Supporting information—This article contains supporting information.

Acknowledgments—We thank Dr Hanchun Yang (China Agricultural University) for PRRSV Abs and Dr Yongchang Cao (Sun Yat-sen University) for the strains of PEDV and PEAV as well as Abs against PEDV-N and PEAV-N. This work was supported by the National Natural Science Foundation of China (grant nos.: 32122082, 32072695, and 31872329) and the Natural Science Foundation of Guangdong Province (grant no.: 2019B1515210024). The funders had no role in study design, data collection and analysis, decision to publish, or preparation of the article.

Author contributions—C. G., Y. C., and X. L. conceptualization; S. H. and H. Z. resources; X. Z. and W. D. investigation; X. Z. and W. D. writing–original draft; X. W. and Z. Z. formal analysis; X. W. and Z. Z. writing–review & editing.

Conflict of interest—The authors declare that they have no conflicts of interest with the contents of this article.

Abbreviations—The abbreviations used are: DED, aspartic acid–glutamic acid–aspartic acid; DMV, double-membrane vesicle; DXD, aspartic acid–any amino acid–aspartic acid; EGFP, enhanced GFP; ER, endoplasmic reticulum; EXT1, exostosin glycosyltransferase 1; HA, hemagglutinin; hpi, hours postinfection; HRP, horseradish peroxidase; HS, heparin sulfate; IP, immunoprecipitation; MOI, multiplicity of infection; nsp, nonstructural protein; PAM, porcine alveolar macrophage; PEAV, porcine enteric alphacoronavirus; PEDV, porcine epidemic diarrhea virus; PRRS, porcine reproductive and respiratory syndrome; PRRSV, porcine reproductive and respiratory syndrome virus; qPCR, quantitative PCR; RIPA, radioimmunoprecipitation assay; RTC, replication transcription complex; TM, transmembrane; Ub, ubiquitin.

References

1. Lunney, J. K., Fang, Y., Ladinig, A., Chen, N., Li, Y., Rowland, B., and Renukaradhya, G. J. (2016) Porcine reproductive and respiratory syndrome virus (PRRSV): Pathogenesis and interaction with the immune system. *Annu. Rev. Anim. Biosci.* **4**, 129–154
2. Goyal, S. M. (1993) Porcine reproductive and respiratory syndrome. *J. Vet. Diagn. Invest.* **5**, 656–664
3. Fang, Y., and Snijder, E. J. (2010) The PRRSV replicase: Exploring the multifunctionality of an intriguing set of nonstructural proteins. *Virus Res.* **154**, 61–76
4. Gorbalenya, A. E., Enjuanes, L., Ziebuhr, J., and Snijder, E. J. (2006) Nidovirales: Evolving the largest RNA virus genome. *Virus Res.* **117**, 17–37
5. Murtaugh, M. P., Stadejek, T., Abrahante, J. E., Lam, T. T., and Leung, F. C. (2010) The ever-expanding diversity of porcine reproductive and respiratory syndrome virus. *Virus Res.* **154**, 18–30
6. Nodelijk, G. (2002) Porcine reproductive and respiratory syndrome (PRRS) with special reference to clinical aspects and diagnosis. A review. *Vet. Q.* **24**, 95–100
7. Du, T., Nan, Y., Xiao, S., Zhao, Q., and Zhou, E. M. (2017) Antiviral strategies against PRRSV infection. *Trends Microbiol.* **25**, 968–979
8. Busse-Wicher, M., Wicher, K. B., and Kusche-Gullberg, M. (2014) The exostosin family: Proteins with many functions. *Matrix Biol.* **35**, 25–33

9. Le Merrer, M., Legeai-Mallet, L., Jeannin, P. M., Horsthemke, B., Schinzel, A., Plauchu, H., Toutain, A., Achard, F., Munnich, A., and Maroteaux, P. (1994) A gene for hereditary multiple exostoses maps to chromosome 19p. *Hum. Mol. Genet.* **3**, 717–722
10. O'Hearn, A., Wang, M., Cheng, H., Lear-Rooney, C. M., Koning, K., Rumschlag-Booms, E., Varhegyi, E., Olinger, G., and Rong, L. (2015) Role of EXT1 and glycosaminoglycans in the early stage of filovirus entry. *J. Virol.* **89**, 5441–5449
11. Savidis, G., McDougall, W. M., Meraner, P., Perreira, J. M., Portmann, J. M., Trincucci, G., John, S. P., Aker, A. M., Renzette, N., Robbins, D. R., Guo, Z., Green, S., Kowalik, T. F., and Brass, A. L. (2016) Identification of Zika virus and dengue virus dependency factors using functional genomics. *Cell Rep.* **16**, 232–246
12. Baggen, J., Persoons, L., Vanstreels, E., Jansen, S., Van Looveren, D., Boeckx, B., Geudens, V., De Man, J., Jochmans, D., Wauters, J., Wauters, E., Vanaudenaerde, B. M., Lambrechts, D., Neyts, J., Dallmeier, K., *et al.* (2021) Genome-wide CRISPR screening identifies TMEM106B as a proviral host factor for SARS-CoV-2. *Nat. Genet.* **53**, 435–444
13. Zhao, C., Liu, H., Xiao, T., Wang, Z., Nie, X., Li, X., Qian, P., Qin, L., Han, X., Zhang, J., Ruan, J., Zhu, M., Miao, Y.-L., Zuo, B., Yang, K., *et al.* (2020) CRISPR screening of porcine sgRNA library identifies host factors associated with Japanese encephalitis virus replication. *Nat. Commun.* **11**, 5178
14. Luteijn, R. D., van Diemen, F., Blomen, V. A., Boer, I. G. J., Manikam Sadasivam, S., van Kuppevelt, T. H., Drexler, I., Brummelkamp, T. R., Lebbink, R. J., and Wiertz, E. J. (2019) A genome-wide haploid genetic screen identifies heparan sulfate-associated genes and the macropinocytosis modulator TMED10 as factors supporting vaccinia virus infection. *J. Virol.* **93**, e02160-18
15. Colley, K. J. (1997) Golgi localization of glycosyltransferases: More questions than answers. *Glycobiology* **7**, 1–13
16. Pedersen, L. C., Dong, J., Taniguchi, F., Kitagawa, H., Krahn, J. M., Pedersen, L. G., Sugahara, K., and Negishi, M. (2003) Crystal structure of an alpha 1,4-N-acetylhexosaminyltransferase (EXTL2), a member of the exostosin gene family involved in heparan sulfate biosynthesis. *J. Biol. Chem.* **278**, 14420–14428
17. Zak, B. M., Crawford, B. E., and Esko, J. D. (2002) Hereditary multiple exostoses and heparan sulfate polymerization. *Biochim. Biophys. Acta* **1573**, 346–355
18. Pohl, C., and Dikic, I. (2019) Cellular quality control by the ubiquitin-proteasome system and autophagy. *Science* **366**, 818–822
19. Zhang, H., Fang, L., Zhu, X., Dang, W., and Xiao, S. (2018) Global analysis of ubiquitome in PRRSV-infected pulmonary alveolar macrophages. *J. Proteomics* **184**, 16–24
20. McCormick, C., Duncan, G., Goutsos, K. T., and Tufaro, F. (2000) The putative tumor suppressors EXT1 and EXT2 form a stable complex that accumulates in the Golgi apparatus and catalyzes the synthesis of heparan sulfate. *Proc. Natl. Acad. Sci. U. S. A.* **97**, 668–673
21. Yang, Y.-L., Yu, J.-Q., and Huang, Y.-W. (2020) Swine enteric alphacoronavirus (swine acute diarrhea syndrome coronavirus): An update three years after its discovery. *Virus Res.* **285**, 198024
22. Nadanaka, S., and Kitagawa, H. (2018) Exostosin-like 2 regulates FGF2 signaling by controlling the endocytosis of FGF2. *Biochim. Biophys. Acta Gen. Subj.* **1862**, 791–799
23. Anderson, D. E., Cui, J., Ye, Q., Huang, B., and Tan, X. (2020) Orthogonal genome-wide screenings in bat cells identify MTHFD1 as a target of broad antiviral therapy. *Proc. Natl. Acad. Sci. U. S. A.* **118**, e2104759118
24. Rascon-Castelo, E., Burgara-Estrella, A., Mateu, E., and Hernandez, J. (2015) Immunological features of the non-structural proteins of porcine reproductive and respiratory syndrome virus. *Viruses* **7**, 873–886
25. Angelini, M. M., Akhlaghpour, M., Neuman, B. W., and Buchmeier, M. J. (2013) Severe acute respiratory syndrome coronavirus nonstructural proteins 3, 4, and 6 induce double-membrane vesicles. *mBio* **4**, e00524-13
26. Arora, S., Yang, J.-M., and Hait, W. N. (2005) Identification of the ubiquitin-proteasome pathway in the regulation of the stability of eukaryotic elongation factor-2 kinase. *Cancer Res.* **65**, 3806–3810
27. Yang, L., Wang, R., Ma, Z., Xiao, Y., Nan, Y., Wang, Y., Lin, S., Zhang, Y.-J., and Lyles, D. S. (2016) Porcine reproductive and respiratory syndrome virus antagonizes JAK/STAT3 signaling via nsp5, which induces STAT3 degradation. *J. Virol.* **91**, e02087-16
28. Gao, J., Xiao, S., Liu, X., Wang, L., Ji, Q., Mo, D., and Chen, Y. (2014) Inhibition of HSP70 reduces porcine reproductive and respiratory syndrome virus replication *in vitro*. *BMC. Microbiol.* **14**, 64
29. Kitagawa, H., Shimakawa, H., and Sugahara, K. (1999) The tumor suppressor EXT-like gene EXTL2 encodes an alpha1, 4-N-acetylhexosaminyltransferase that transfers N-acetylgalactosamine and N-acetylglucosamine to the common glycosaminoglycan-protein linkage region. The key enzyme for the chain initiation of heparan sulfate. *J. Biol. Chem.* **274**, 13933–13937
30. Prydz, K. (2015) Determinants of glycosaminoglycan (GAG) structure. *Biomolecules* **5**, 2003–2022
31. Hirschberg, C. B., and Snider, M. D. (1987) Topography of glycosylation in the rough endoplasmic reticulum and Golgi apparatus. *Annu. Rev. Biochem.* **56**, 63–87
32. Silbert, J. E., and Sugumaran, G. (1995) Intracellular membranes in the synthesis, transport, and metabolism of proteoglycans. *Biochim. Biophys. Acta* **1241**, 371–384
33. Guo, C., Cong, P., He, Z., Mo, D., Zhang, W., Chen, Y., and Liu, X. (2015) Inhibitory activity and molecular mechanism of protegrin-1 against porcine reproductive and respiratory syndrome virus *in vitro*. *Antivir. Ther.* **20**, 573–582
34. Guo, C., Huang, Y., Cong, P., Liu, X., Chen, Y., and He, Z. (2014) Cecropin P1 inhibits porcine reproductive and respiratory syndrome virus by blocking attachment. *BMC. Microbiol.* **14**, 273
35. Wang, C., Huang, B., Kong, N., Li, Q., Ma, Y., Li, Z., Gao, J., Zhang, C., Wang, X., Liang, C., Dang, L., Xiao, S., Mu, Y., Zhao, Q., Sun, Y., *et al.* (2013) A novel porcine reproductive and respiratory syndrome virus vector system that stably expresses enhanced green fluorescent protein as a separate transcription unit. *Vet. Res.* **44**, 104